

# Novel inhibitors of RANKL-induced osteoclastogenesis: Design, synthesis, and biological evaluation of 6-(2,4-difluorophenyl)-3-phenyl-2H-benzo[e][1,3]oxazine-2,4(3H)-diones



Chia-Chung Lee<sup>a,b,c</sup>, Fei-Lan Liu<sup>d</sup>, Chun-Liang Chen<sup>a</sup>, Tsung-Chih Chen<sup>a</sup>, Feng-Cheng Liu<sup>e</sup>, Ahmed Atef Ahmed Ali<sup>b,f</sup>, Deh-Ming Chang<sup>b,d,\*</sup>, Hsu-Shan Huang<sup>a,b,c,\*</sup>

<sup>a</sup> Graduate Institute of Cancer Biology and Drug Discovery, College of Medical Science and Technology, Taipei Medical University, Taipei 110, Taiwan, ROC

<sup>b</sup> Graduate Institute of Life Sciences, National Defense Medical Center, Taipei 114, Taiwan, ROC

<sup>c</sup> School of Pharmacy, National Defense Medical Center, Taipei 114, Taiwan, ROC

<sup>d</sup> Rheumatology/Immunology/Allergy, Taipei Veterans General Hospital, Taipei 112, Taiwan, ROC

<sup>e</sup> Rheumatology/Immunology/Allergy, Tri-Service General Hospital, National Defense Medical Center, Taipei 114, Taiwan, ROC

<sup>f</sup> Taiwan International Graduate Program, Molecular and Cell Biology Program, Institute of Molecular Biology, Academia Sinica, Taipei 115, Taiwan, ROC

## ARTICLE INFO

### Article history:

Received 26 April 2015

Revised 2 June 2015

Accepted 3 June 2015

Available online 10 June 2015

### Keywords:

NDMC101

Osteoclastogenesis

RANKL

TRAP-staining assay

Pit formation assay

## ABSTRACT

A series of novel 6-(2,4-difluorophenyl)-3-phenyl-2H-benzo[e][1,3]oxazine-2,4(3H)-dione derivatives were synthesized and evaluated for their inhibitory effects on osteoclast activities by using TRAP-staining assay. Among the tested compounds, **3d** and **3h** exhibited more potent osteoclast-inhibitory activities than the lead compound NDMC503 (a ring-fused structure of NDMC101), as reported in our previous study. Both **3d** and **3h** exhibited two-fold increase in activity compared to NDMC503. In addition, our biological results indicated that **3d** and **3h** could suppress RANKL-induced osteoclastogenesis-related marker genes, such as *NFATc1*, *c-fos*, *TRAP*, and *cathepsin K*. Notably, **3d** could significantly attenuate the bone-resorbing activity of osteoclasts in the pit formation assay. Thus, this study might provide a new class of lead structures that warrant further development as potential anti-resorptive agents.

© 2015 Elsevier Ltd. All rights reserved.

## 1. Introduction

Bone remodeling is a dynamic process that is mediated by the balance between bone formation and resorption, which are regulated by osteoblasts and osteoclasts, respectively.<sup>1–3</sup> When the balanced bone remodeling is disturbed in favor of bone resorption, it will lead to pathological diseases, such as osteoporosis<sup>4,5</sup> and rheumatoid arthritis (RA).<sup>6–8</sup> Osteoclasts are multinucleated cells (MNCs) originating from fusion of the monocyte/macrophage hematopoietic lineage mononuclear progenitors.<sup>9–12</sup> The receptor activator of nuclear factor κB ligand (RANKL) is a member of the tumor necrosis factor (TNF) family and is an essential factor for osteoclast differentiation.<sup>13–15</sup> Through the activation of RANKL–RANK signaling transduction cascades, TNF receptor-associated factor 6 (TRAF 6) is recruited to the intracellular domain of RANK and triggers various downstream signaling, including the

transcription factors NF-κB and nuclear factor of activated T cells c1 (NFATc1) pathways.<sup>16,17</sup> Among these factors, both NF-κB and NFATc1 play essential roles in controlling excessive osteoclast differentiation and activation.<sup>18–20</sup> Furthermore, it was found that RANKL signaling is associated with the expression of osteoclast-associated genes such as *NFATc1*,<sup>18–20</sup> *c-fos*,<sup>21,22</sup> *tartrate-resistant acid phosphatase (TRAP)*,<sup>23,24</sup> *cathepsin K*,<sup>25,26</sup> *matrix metalloproteinase-9 (MMP-9)*,<sup>27,28</sup> and *dendritic cell-specific transmembrane protein (DC-STAMP)*.<sup>29,30</sup> Based on these mechanistic findings, we conclude that osteoclast differentiation in RANKL–RANK signaling pathway provides potential molecular targets for the development of anti-resorptive agents.

In clinical trials, bisphosphonates are widely used as therapeutic agents for bone loss by inhibiting excessive osteoclast formation and activation.<sup>31–33</sup> However, bisphosphonates may cause some adverse gastrointestinal effects, osteonecrosis of jaw, and renal toxicity.<sup>34–36</sup> Hence, numerous natural products and synthetic small molecules have been found to be potential inhibitors of osteoclastogenesis, such as Paeonol,<sup>37</sup> Genistein,<sup>38</sup> Daidzein,<sup>39</sup> Magnolol,<sup>40</sup> NDMC101,<sup>41,42</sup> NDMC503,<sup>42</sup> and ABD345 (Fig. 1).<sup>43</sup> In our previous work, we developed a salicylanilide-derived synthetic

\* Corresponding authors. Tel.: +886 2 275 7799; fax: +886 2 7735 1333 (D.-M.C.); tel.: +886 2 2736 1661x7525; fax: +886 2 6638 7537 (H.-S.H.).

E-mail addresses: [ming0503@ms3.hinet.net](mailto:ming0503@ms3.hinet.net) (D.-M. Chang), [huanghs99@tmu.edu.tw](mailto:huanghs99@tmu.edu.tw) (H.-S. Huang).

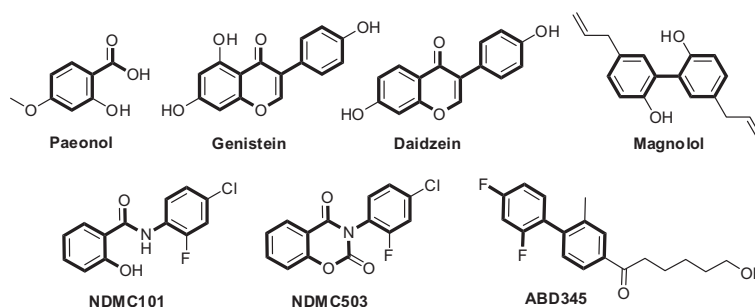


Figure 1. Chemical structures of osteoclast inhibitors in literatures.

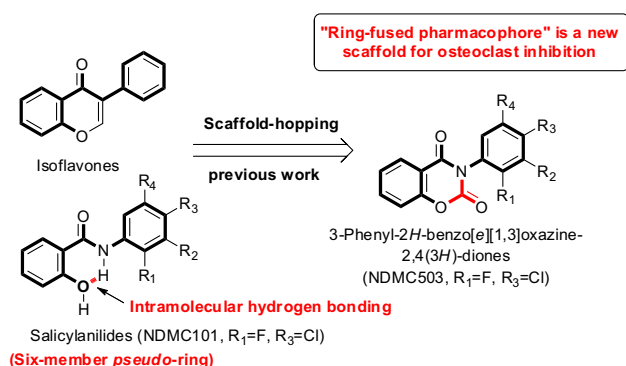


Figure 2. The essential pharmacophore for osteoclast inhibition.

small molecule (NDMC101) that not only inhibited the RANKL-induced osteoclastogenesis by suppressing NFATc1 and NF- $\kappa$ B activity, but also significantly reduced the number of TRAP-staining osteoclasts at sites of articular bone erosions in collagen-induced arthritis (CIA) mice.<sup>41</sup> On the basis of these findings, the lead structure of NDMC101 can be considered as an osteoclastogenesis inhibitor that warrants further lead optimization. Therefore, we developed a series of 3-phenyl-2H-benzo[e][1,3]oxazine-2,4(3H)-dione derivatives by scaffold hopping strategy, as reported in our previous study (Fig. 2).<sup>42</sup> We also found that rigidifying the *pseudo* six-membered ring of salicylanilide core may increase the anti-resorptive activity.<sup>42</sup> Compared to the lead structure NDMC101, we found that the ring-fused pharmacophore of NDMC503 exhibited

higher inhibitory effects on the RANKL-induced osteoclastogenesis.<sup>42</sup> On the basis of our previous structure–activity relationships (SARs) studies, the scaffold of 3-phenyl-2H-benzo[e][1,3]oxazine-2,4(3H)-dione can be considered as an essential pharmacophore for the development of osteoclast inhibitors. Recently, van't Hof developed a series of biphenyl-based derivatives including the 2',4'-difluorobiphenyl pharmacophore, as inhibitors of the RANKL-induced osteoclastogenesis which exhibited anti-resorptive effects *in vitro* and *in vivo*.<sup>43–49</sup> These observations along with our previous promising results initiated quest for the development of a new class of anti-resorptive agents.

Considering the importance of the ring-fused pharmacophore and the 2',4'-difluorobiphenyl group in the development of new class of anti-resorptive agents, a series of 6-(2,4-difluorophenyl)-3-phenyl-2H-benzo[e][1,3]oxazine-2,4(3H)-diones (**3a–3l**) were designed and synthesized in the present work (Fig. 3). The inhibitory effects of synthesized compounds (**3a–3l**) on RANKL-induced osteoclast differentiation and formation were evaluated using the TRAP-staining assay. On the basis of these screening results, we constructed the SARs of all compounds according to the inhibition of RANKL-induced osteoclastogenesis. Among our new synthesized series, compounds **3d** and **3h** were the most potent derivatives that effectively inhibited the RANKL-induced osteoclastogenesis. To further investigate the inhibitory effects of compounds **3d** and **3h** on the activation of RANKL–RANK signaling transduction cascades, we tested the effects of both compounds on the RANKL-induced osteoclastogenesis through suppressing the osteoclastogenesis-related marker genes, blocking the NF- $\kappa$ B nuclear translocation, and decreasing the NFATc1 expression levels. Detailed illustration of the biological experiments performed to evaluate compounds **3d** and **3h** is presented as follows.

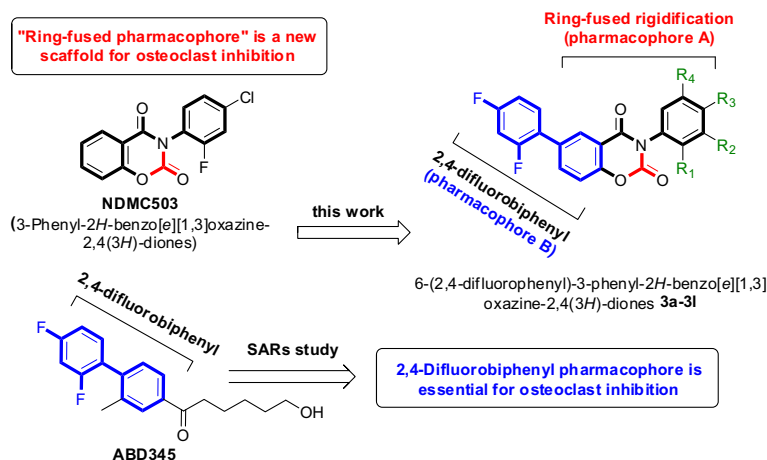
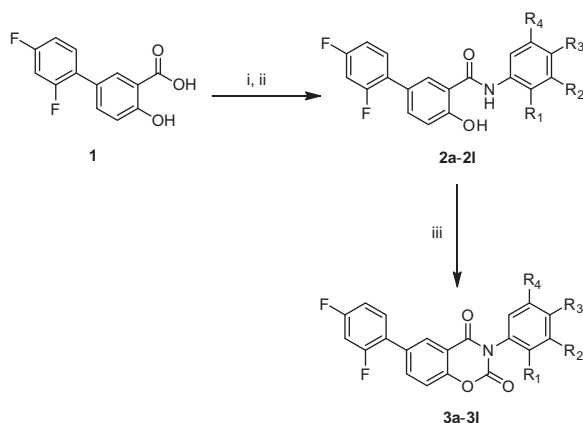


Figure 3. Rational design, SARs study, and the essential pharmacophore for the development of 6-(2,4-difluorophenyl)-3-phenyl-2H-benzo[e][1,3]oxazine-2,4(3H)-diones (**3a–3l**).



**Scheme 1.** Synthetic routes of 6-(2,4-difluorophenyl)-3-phenyl-2H-benzo[e][1,3]oxazine-2,4(3H)-diones (**3a–3l**). Reagents and conditions: (i) SOCl<sub>2</sub>, anhydrous THF, reflux, 6 h; (ii) anilines, anhydrous THF, reflux, 12–14 h; (iii) methyl chloroformate, anhydrous THF/pyridine, reflux, 2 h.

## 2. Chemical synthesis

In the present work, it is noteworthy to mention that this study is the first to use 2',4'-difluoro-4-hydroxybiphenyl-3-carboxylic acid (diflunisal) as starting material for the synthesis of a series of 6-(2,4-difluorophenyl)-3-phenyl-2H-benzo[e][1,3]oxazine-2,4(3H)-diones. Diflunisal is approved worldwide for the treatment of inflammatory diseases.<sup>50,51</sup> As part of an endeavor to profile the potential therapeutics for the treatment of inflammation-related bone diseases, diflunisal is an attractive scaffold that justifies further structure modification. Thus, diflunisal (**1**) was used as our starting material that was transformed to the corresponding acid chloride after treatment with thionyl chloride, and then the acid chloride was reacted with the substituted anilines to give the corresponding compounds (**2a–2l**). We further cyclized compounds (**2a–2l**) to the corresponding cyclic compounds (**3a–3l**) by using methyl chloroformate as cyclization reagent in the presence of pyridine and tetrahydrofuran (THF).<sup>52</sup> The reaction mixtures were refluxed over 70 °C for 2 h and then stirred for another 12 h at room temperature. The mixture solution was acidified with 5% hydrochloric acid and was put in ice bath to obtain compounds (**3a–3l**) in 11–61% yields (see [Scheme 1](#)). The

**Table 1**

Effects of 6-(2,4-difluorophenyl)-3-phenyl-2H-benzo[e][1,3]oxazine-2,4(3H)-diones on RANKL-induced osteoclastogenesis and cell viability in RAW264.7 cells

Compound	Substituent				% inhibition of MNC <sup>a</sup>	% cell viability <sup>b</sup>
	R <sub>1</sub>	R <sub>2</sub>	R <sub>3</sub>	R <sub>4</sub>		
<b>3a</b>	F	H	Cl	H	19.41 ± 1.40	96.22 ± 0.53
<b>3b</b>	F	H	F	H	42.32 ± 6.62	96.49 ± 1.86
<b>3c</b>	H	F	F	H	17.35 ± 7.49	72.15 ± 0.43
<b>3d</b>	F	H	H	F	86.84 ± 1.74	86.60 ± 5.69
<b>3e</b>	CF <sub>3</sub>	H	H	H	31.58 ± 4.00	95.53 ± 3.86
<b>3f</b>	H	CF <sub>3</sub>	H	H	62.92 ± 2.65	100.13 ± 0.94
<b>3g</b>	H	H	CF <sub>3</sub>	H	16.85 ± 4.61	103.01 ± 2.51
<b>3h</b>	H	CCH	H	H	57.46 ± 3.25	88.38 ± 4.65
<b>3i</b>	H	CN	H	H	33.99 ± 6.98	102.79 ± 1.93
<b>3j</b>	H	H	CN	H	29.44 ± 5.48	108.33 ± 1.10
<b>3k</b>	H	OCH <sub>3</sub>	OCH <sub>3</sub>	H	21.20 ± 2.49	103.05 ± 4.03
<b>3l</b>	H	OCH <sub>3</sub>	H	H	30.75 ± 5.77	105.53 ± 4.7

<sup>a</sup> RAW 264.7 cells, the cells were cultured in the maintaining mediums and RANKL (100 ng/mL) with or without the tested compound (5 μM) for 4 days. TRAP-positive multinucleated cells (MNCs) were counted as osteoclasts (three or more than three nuclei ( $N > 3$ )). RANKL-induced osteoclast differentiation is shown as relative activity (% of RANKL-treated with compounds/RANKL-treated without compounds as vehicle). Inhibition (%) = 100% – MNCs (%) of compounds.

<sup>b</sup> Cell viability of tested compounds were determined relative to the control at 5 μM by MTT assay. All representative data were performed the means ± SD at least three times independently ( $n > 3$ ).

byproducts were separated and purified by employing their different physicochemical properties using recrystallization and chromatography procedures. The purity of all synthetic compounds was more than 95%. The structures of all synthesized compounds are elucidated along with their spectroscopic characterizations in the experimental section. In addition, the ring-fused structure of **3h** was further confirmed by using the single-crystal X-ray crystallography (the ORTEP plot of **3h** is presented in [Fig. 4](#)).

## 3. Biological results and discussion

### 3.1. Effects of the synthesized compounds on the RANKL-induced osteoclast differentiation

RAW264.7 cells (osteoclast precursor cells) are widely used as an osteoclast differentiation model.<sup>41,53</sup> The TRAP enzyme is highly expressed in osteoclasts and the histochemical staining of TRAP-positive MNCs is widely used to identify osteoclasts both in vivo

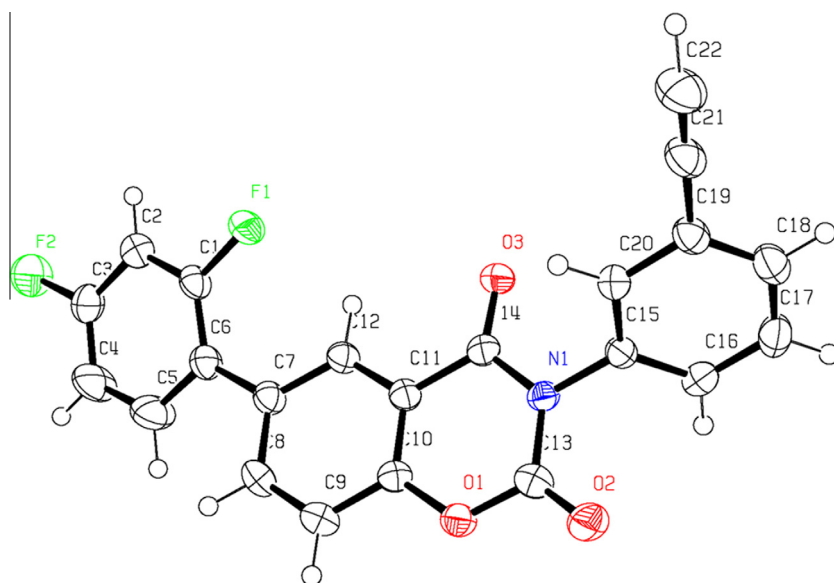


**Figure 4.** ORTEP diagram of **3h**. Ellipsoids are drawn at 50% probability level; selected crystallographic data for **3h** are given in [Supplementary data](#).

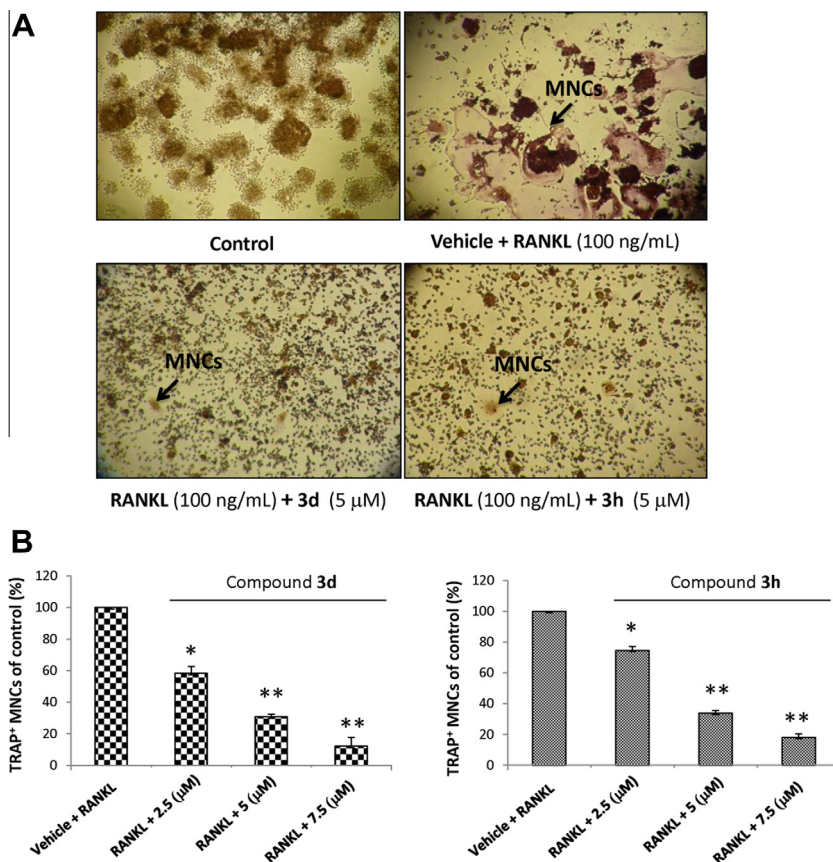


**Figure 5.** Effects of compounds **3d** and **3h** on the RANKL-induced osteoclastogenesis from RAW264.7 cells by using TRAP-staining activity assay. (A) Control group was cultured without test compounds in the absence of RANKL (100 ng/mL). Vehicle was cultured without the tested compounds and RAW264.7 cells were cultured with **3d** and **3h** at 5  $\mu$ M in the presence of RANKL. After 4 days, the mature osteoclasts were fixed and stained by TRAP. The TRAP-positive MNCs containing more than three nuclei ( $N > 3$ ) were visualized by light microscopy. (B) Vehicle was cultured without the tested compounds and RAW264.7 cells were cultured with **3d** and **3h** at 7.5, 5, and 2.5  $\mu$ M in the presence of RANKL. RANKL-induced osteoclast differentiation is shown as relative activity (% of RANKL-treated with compounds/RANKL-treated without compounds as vehicle). All data were performed the means  $\pm$  SD at least three times independently; \* $P < 0.05$  and \*\* $P < 0.01$  compared with the RANKL-treated group.

and in vitro.<sup>54</sup> The inhibitory activities of all synthesized compounds (**3a–3l**) on the RANKL-induced TRAP-positive MNCs from RAW264.7 cells were screened using the TRAP-staining assay. Almost all of final compounds (**3a–3l**) did not affect the viability of RAW264.7 cells (Table 1). These observations prove that their inhibitory activities were not due to their cytotoxic effects. As illustrated in Table 1, most of our synthesized compounds decreased the percentage of TRAP-positive MNCs at a concentration of 5  $\mu$ M. The highest percent inhibition values of MNCs were for compounds **3d**, **3f**, and **3h** at 5  $\mu$ M ( $86.84 \pm 1.74\%$ ,  $62.92 \pm 2.65\%$ , and  $57.46 \pm 3.25\%$ , respectively). Compared to compounds **3d**, **3f**, and **3h**, NDMC503 (a ring-fused structure of NDMC101) exhibited lower inhibitory effect ( $25.38 \pm 11.63\%$ ) on the TRAP-positive staining MNCs at a concentration of 5  $\mu$ M in our previous study.<sup>42</sup> In order to investigate whether these compounds inhibited the activity of osteoclasts, the inhibitory effects of compounds **3d**, **3f**, and **3h** on RANKL-induced TRAP activity were determined. Compounds **3d**, **3f**, and **3h** were found to dose-dependently suppress RANKL-induced TRAP activity with  $IC_{50}$  values of 4.31, 4.29, and 3.7  $\mu$ M, respectively (as shown in Supplementary data). Based on the results of TRAP-staining assay and TRAP activity, we conclude that our new 6-(2,4-difluorophenyl)-3-phenyl-2H-benzo[e][1,3]oxazine-2,4(3H)-diones **3d** and **3h** are potent inhibitors of RANKL-induced osteoclastogenesis. Both compounds **3d** and **3h** were able to reduce the number of TRAP-positive MNCs at 5  $\mu$ M as shown in Figure 5A and B.

On the basis of these screening results, the SARs of compounds **3a–3l** are briefly summarized as follows. Amongst compounds

bearing mono-substitution at the aniline moiety, we found that the substitution at  $R_2$  position showed relatively higher activities than those at  $R_1$  or  $R_3$  position, especially for 3-ethynyl aniline. Amongst compounds bearing difluoro groups at the aniline moiety and their cyclic analogs, we observed that the 2,5-difluoro analogs showed relatively higher activities than the 2,4-difluoro and 3,4-difluoro analogs. Based on these SARs observations, it is confirmed that the 6-(2,4-difluorophenyl)-3-phenyl-2H-benzo[e][1,3]oxazine-2,4(3H)-dione derivatives can increase in the inhibitory activity of RANKL-induced osteoclastogenesis, especially for **3d** and **3h**. Thus, we chose both compounds which were the most potent among the synthesized series for further mechanistic investigation in the RANKL/RANK signaling pathway.

### 3.2. Effects of **3d** and **3h** on the expression levels of osteoclastogenesis-related marker genes during the RANKL-induced osteoclast formation

Osteoclast differentiation is associated with up-regulation of osteoclastogenesis-related marker genes such as *NFATc1*, *c-fos*, *TRAP*, *cathepsin K*, *MMP-9*, and *DC-STAMP* in response to the binding of RANKL to RANK.<sup>55,56</sup> In order to test whether compounds **3d** and **3h** would regulate the expression levels of osteoclastic genes during the RANKL-induced osteoclastogenesis, we assessed the inhibitory effects of **3d** and **3h** on the expression levels of *NFATc1*, *c-fos*, *TRAP*, *cathepsin K*, *MMP-9*, and *DC-STAMP* genes by using the reverse transcription polymerase chain reaction (RT-PCR) assay. Our results showed that the expression levels of *NFATc1*, *c-fos*,

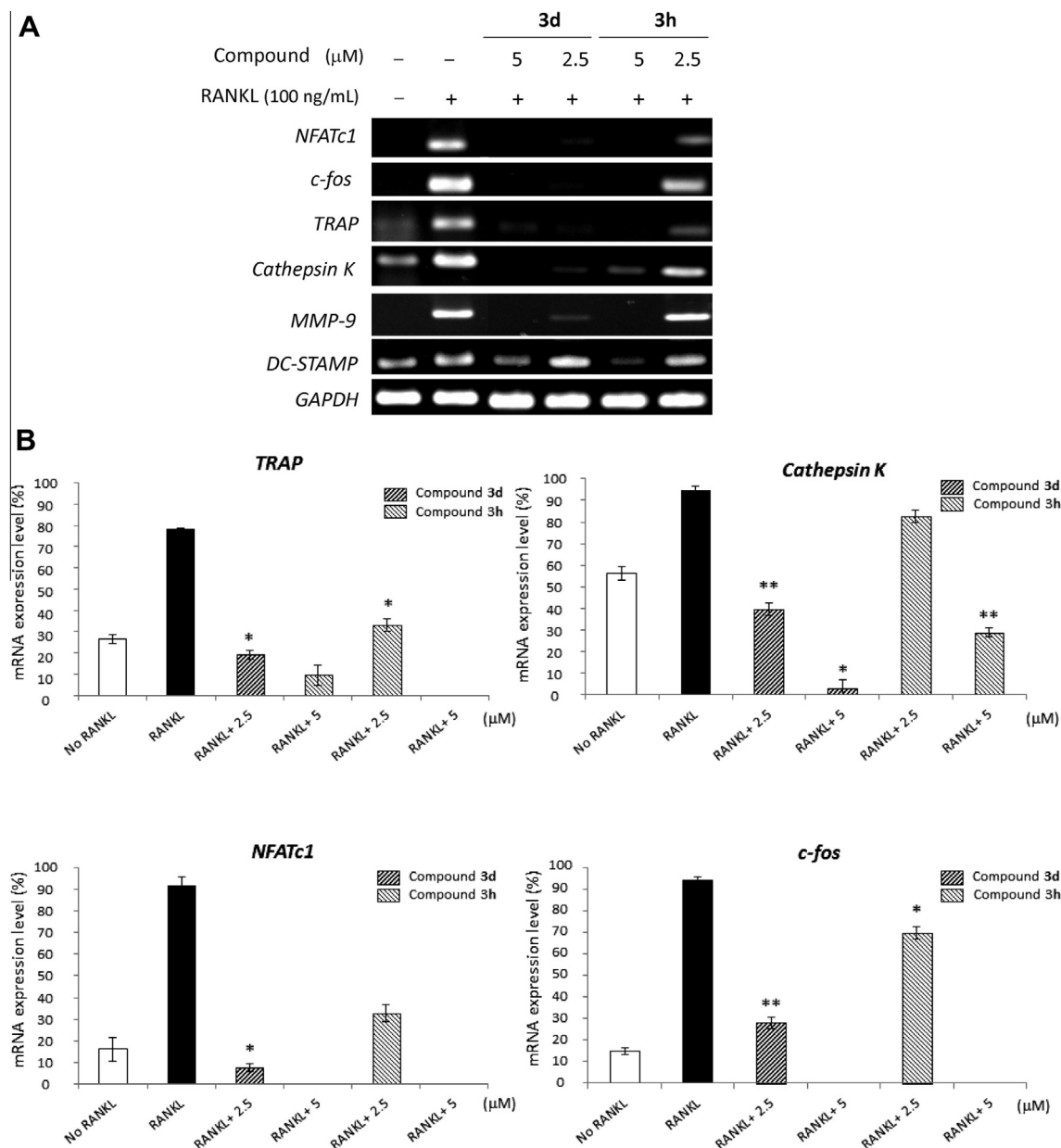


**Figure 6.** Effects of compounds **3d** and **3h** on the RANKL-induced osteoclastogenesis-related gene expression levels. (A) RAW264.7 cells were either pretreated or not with **3d** and **3h** at 5  $\mu\text{M}$  for 1 h and then treated with RANKL (100 ng/mL) for 24 h. Total RNA was isolated with TRIzol, and 2  $\mu\text{g}$  of total RNA was used to transcribe cDNA. cDNA was used as a template for PCR with mouse-specific primers. (B) Effects of compounds **3d** and **3h** on the RANKL-induced osteoclastogenic mRNA expression levels were normalized as relative activity (% of control). All data were performed the means  $\pm$  SD at least two times independently; \* $P$  < 0.05 and \*\* $P$  < 0.01 compared with the RANKL-treated group.

TRAP, cathepsin K, MMP-9, and DC-STAMP were increased in response to RANKL stimulation for 24 h (Fig. 6A). However, such levels including NFATc1, c-fos, TRAP, and cathepsin K were significantly suppressed after treatment with **3d** and **3h** at concentrations of 2.5 and 5  $\mu\text{M}$  (Fig. 6B). These results revealed that compounds **3d** and **3h** might decrease the RANKL-induced mRNA expression levels in response to inhibiting RANK signaling pathway.

### 3.3. Effects of **3d** and **3h** on the RANKL-induced NF- $\kappa$ B activation and NFATc1 expression levels in the nucleus during osteoclast differentiation

Some master transcriptional factors can be activated and are responsible for promoting osteoclastogenesis-related marker

genes through a mechanism dependent on RANKL–RANK interaction.<sup>55,56</sup> For example, NF- $\kappa$ B and NFATc1 are essential transcriptional factors for the osteoclast differentiation and formation.<sup>18,57</sup> However, they are not activated within the same time frame. NF- $\kappa$ B is an early-response factor and NFATc1 is a late-response factor.<sup>57</sup> In addition, it has been reported that NF- $\kappa$ B is an upstream transcriptional factor which can modulate NFATc1 expression. In the inactive state, NF- $\kappa$ B is retained in the cytoplasm. When activated, NF- $\kappa$ B would translocate from the cytoplasm into the nucleus. Initially, we examined the inhibitory effects of compounds **3d** and **3h** on the RANKL-stimulated nuclear expression levels of NF- $\kappa$ B in RAW264.7 cells by using NF- $\kappa$ B activity assay. This assay is used to analyze the NF- $\kappa$ B activity through using enzyme-linked immunosorbent assay plates. Compared to the nuclear expression levels in the untreated cells, the

accumulation of NF- $\kappa$ B was increased after treatment with RANKL (Fig. 7A). However, such elevated levels of the nuclear NF- $\kappa$ B were reduced by treatment with the tested compounds, especially for **3d**.

To further confirm the above results, we tested the inhibitory effects of **3d** on the RANKL-induced NF- $\kappa$ B and NFATc1 expression levels in nuclear extracts using Western blotting assay. The data are expressed as the ratios of the protein levels of NF- $\kappa$ B and NFATc1 normalized to the level of TATA-box binding protein (TBP). As shown in Figure 7B, the expression levels of NF- $\kappa$ B and NFATc1 in nuclear extracts increased by RANKL treatment. However, such elevated levels were reduced by treatment with **3d**. These results showed that **3d** might suppress the RANKL-induced NF- $\kappa$ B activation and NFATc1 expressions in nucleus.

### 3.4. Effects of **3d** on the RANKL-induced bone-resorbing activity of osteoclasts

In order to investigate whether compound **3d** would attenuate the bone-resorbing activity of osteoclasts, the pit formation assay was used for evaluating the effect of **3d** on dentine slices. This assay is based on the facts that bone resorption is a characteristic feature of functional osteoclasts, and RANKL induces the bone-

resorbing activity of mature osteoclasts through RANKL–RANK interaction. In this assay, RAW264.7 cells are seeded on dentine slices and then differentiated into mature osteoclasts in response to RANKL stimulation. Resorbing pits were formed on the dentine slices by mature osteoclasts. However, dose-dependent attenuation of the resorbed areas could be observed after treatment with various concentrations of **3d**. Our results showed that **3d** might reduce osteoclast formation by ameliorating RANKL-induced bone-resorbing activity of mature osteoclasts at concentrations of 2.5, 5, and 7.5  $\mu$ M (Fig. 8).

## 4. Conclusions

In a continuous interest in the synthesis of new class of anti-resorptive agents, a series of 6-(2,4-difluorophenyl)-3-phenyl-2H-benzo[e][1,3]oxazine-2,4(3H)-dione derivatives were developed and evaluated for their inhibitory activities on the RANKL-induced osteoclast formation. The general SARs were established by using TRAP-staining assay. These SARs was outlined as follows: (a) compounds bearing mono-substituted groups at R<sub>2</sub> position had higher activities than those at R<sub>1</sub> or R<sub>3</sub> positions at the aniline moiety, especially for 3-ethynyl aniline; (b) compounds bearing di-substituted groups at the aniline moiety revealed that difluoro groups showed relatively higher inhibitory activities, especially for the 2,5-difluoro analogs. Our biological results indicated that compound **3d** exhibited the most potent inhibitory activity towards the RANKL-induced osteoclastogenesis. The proposed mechanism of this activity is shown in Figure 9.

The inhibitory activities of **3d** might be affected by inhibiting NF- $\kappa$ B transcriptional activation and suppressing NFATc1-regulated osteoclastogenesis-related genes. Furthermore, the pit formation assay showed that **3d** could reduce the bone-resorbing activity of mature osteoclasts. This study provides a new class of 6-(2,4-difluorophenyl)-3-phenyl-2H-benzo[e][1,3]oxazine-2,4(3H)-diones as potent anti-resorptive agents for the treatment of bone disorders characterized by excessive osteoclastic resorption.

## 5. Materials and methods

### 5.1. Chemistry

Unless otherwise stated, all materials used were commercially available. Chemical reagents and solvents were purchased from Aldrich and Merck without further purification. Reactions requiring anhydrous conditions were performed in oven-dried glassware and cooled under nitrogen atmosphere. Melting points were determined by a Büchi B-545 melting point apparatus and are uncorrected. Analytical thin layer chromatography was performed with E. Merck silica gel 60 F<sub>254</sub>. <sup>1</sup>H nuclear magnetic resonance (NMR) and <sup>13</sup>C NMR spectra were recorded on Varian Gemini 300 (300 MHz) and Agilent 400 MR DD2 (400 MHz).  $\delta$  value is presented in parts per million (ppm) relative to TMS as an internal standard (0 ppm). Multiplicities were recorded as singlet (s), doublet (d), triplet (t), quartet (q), and double of doublet (dd). Coupling constants (*J*) are expressed in Hz. High resolution mass spectra (HRMS) were measured by Finnigan MAT-95XL (high resolution electron impact ionization, HREI) and Finnigan MAT-95S (high resolution electrospray ionization, HRESI). Spectral data are recorded as *m/z* values. The purity of all synthetic compounds was analyzed by reverse-phase high performance liquid chromatography (HPLC) analysis to be >95%. HPLC spectra for all compounds were acquired using a Hitachi L-2000 series system with UV detector (L-2400, Hitachi). The retention time (*t<sub>r</sub>*) is expressed in min at UV detection of 208 nm. By using HPLC analysis, chromatography

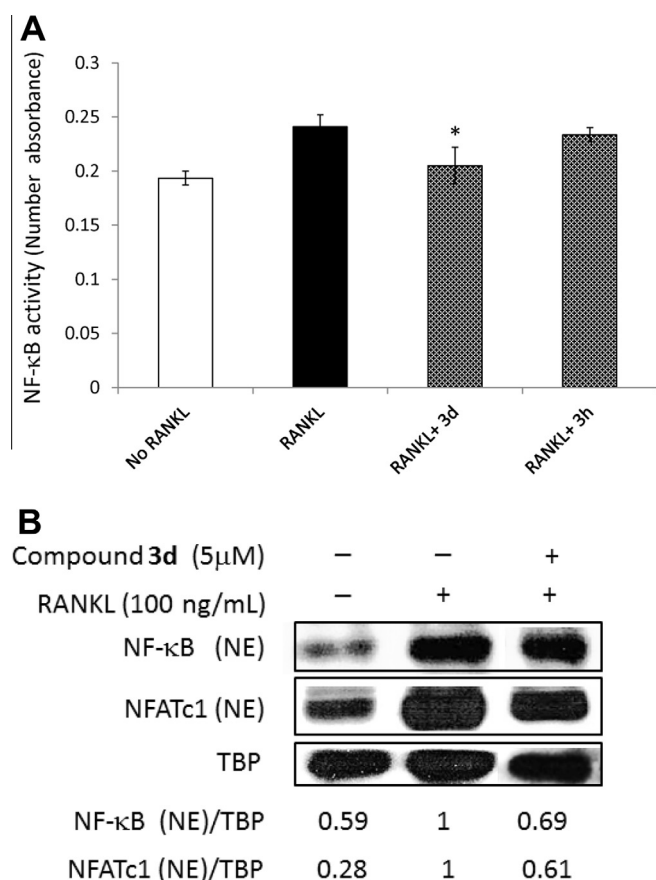


**Figure 7.** (A) Effects of compounds **3d** and **3h** on the RANKL-induced NF- $\kappa$ B expression levels in nucleus. RAW264.7 cells were pretreated with **3d** and **3h** at 5  $\mu$ M for 1 h prior to treatment with RANKL (100 ng/mL) for 24 h. The data represent more than two cultures ( $n > 2$ ); \* $P < 0.05$ , \*\* $P < 0.01$ , significantly different from values after treatment with RANKL along. (B) Effect of **3d** on RANKL-induced nuclear expression levels of NF- $\kappa$ B and NFATc1. RAW264.7 cells treated without RANKL (100 ng/mL) and test compounds as control. Nuclear extracts (NE) were analyzed by using Western blotting employing antibodies to NFATc1 and NF- $\kappa$ B proteins. Equal amounts of proteins were loaded in each lane as demonstrated by the level of TATA-box protein (TBP). All representative data were performed the results at least two times independently.

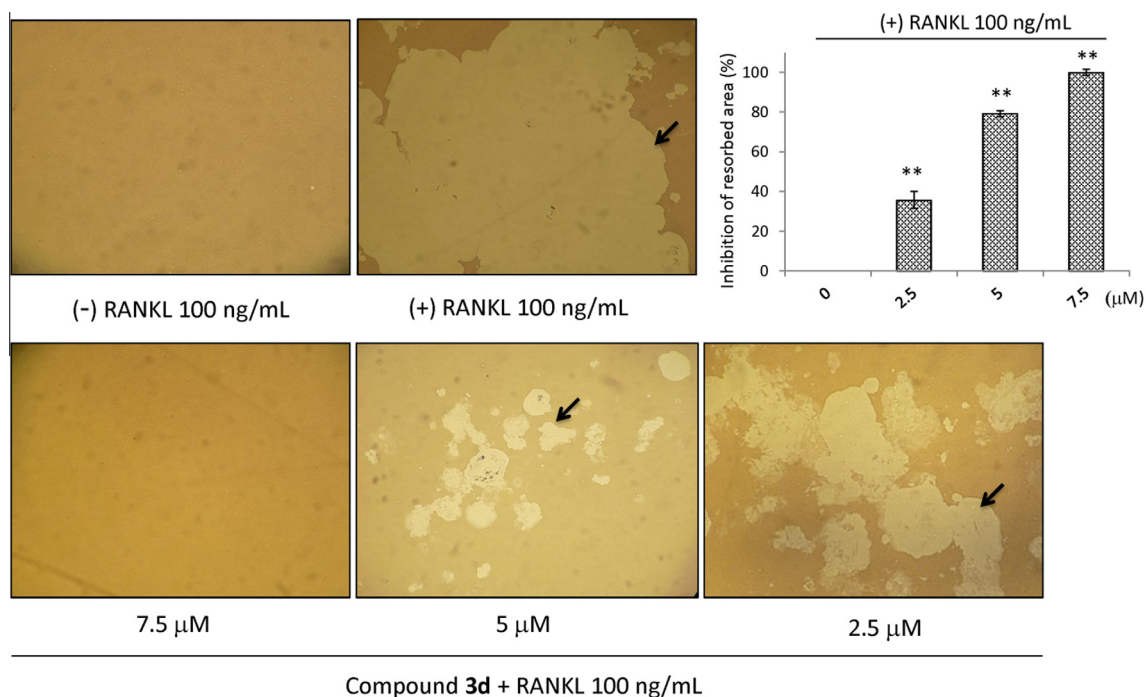


**Figure 8.** Effect of compound **3d** on the bone-resorbing activity of mature osteoclasts. RAW264.7 cells were cultured on bone slices with **3d** at different concentrations (7.5, 5, and 2.5  $\mu\text{M}$ ) in the presence of RANKL (100 ng/mL). After 4 days, the dentine slices were recovered for staining with 0.1% toluidine blue to visualize the resorption pits; arrows indicate pit area; RAW264.7 cells were cultured on bone slices with **3d** at 7.5, 5, and 2.5  $\mu\text{M}$  in the presence of RANKL. Percentages (%) of the resorbed area were determined using ImageJ software and then normalized as relative activity (% of control). Data represent the means  $\pm$  SD of more than 6 slices;  $^*P < 0.05$  and  $^{**}P < 0.01$  compared with the RANKL-treated group.

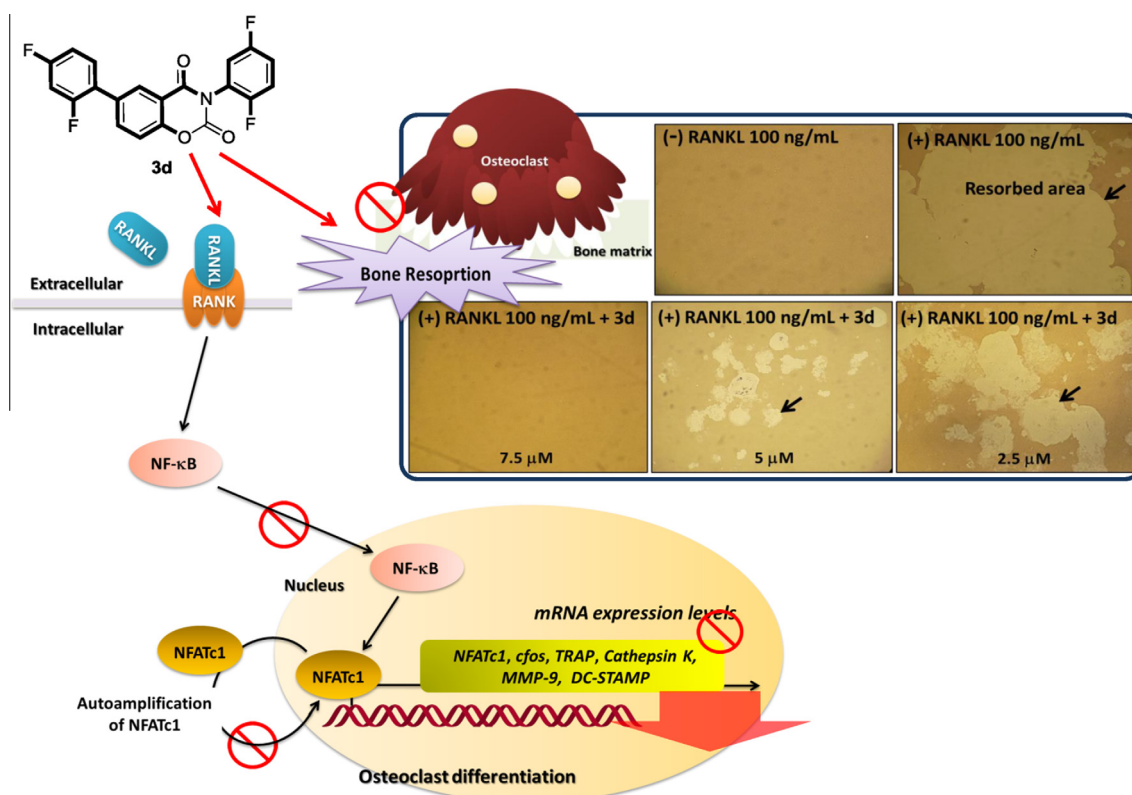


**Figure 9.** Proposed mechanism for the inhibition of RANKL-induced osteoclastogenesis and bone resorption by compound **3d** includes direct effects on NF- $\kappa$ B activation and NFATc1-regulated osteoclastogenesis-related marker genes.

**Table 2**  
Primers used for RT-PCR

Target gene	Forward primer sequence (5'–3')	Reverse primer sequence (5'–3')
<i>Cathespin K</i>	AGGCAGCTAAATGCAGAGGGTA	CAGGCGTTGTCTTATTCGGAG
<i>c-fos</i>	GGTTCAACGCCGACTACGAG	CTGACACGGTCTTACCATTCC
<i>DCSTAMP</i>	CCGCTGTGGACTATCTGCTGTA	TTCCCGTCAGCCTCTCAAT
<i>GAPDH</i>	GTGAGGCCGGTGTGAGTATGT	ACAGTCTCTGGGTGGCAGTGT
<i>TRAP</i>	ACGGCTACTTGCGGTTTCACTA	GTGTGGGCATACCTTCTTCTGT
<i>MMP-9</i>	AGGCCTCTACAGAGTCTTTG	CAGTCCAACAAGAAAGGACG
<i>NFATc1</i>	CCCTGACCACCGATAGCACTCT	GGTGCCTTCCGCTCATAGTG

performed on a C18 reverse-phase column (XBridge Shield RP18 Column, 130 Å, 5 µm, 4.6 mm × 250 mm, Waters). A flow rate of 1.0 mL/min was used with a mobile phase gradient of 0–20% H<sub>2</sub>O in MeOH.

## 5.2. X-ray crystallography

A single crystal of suitable size for X-ray diffractometry was selected under a microscope and mounted on the tip of a glass fiber, which was positioned on a copper pin. Crystallographic assay was performed as described in the reported protocol.<sup>58,59</sup> The X-ray data for **3d** was collected with a Bruker Kappa CCD diffractometer, employing graphite-monochromated Mo-K $\alpha$  radiation at 200 K and the  $\theta$ – $2\theta$  scan mode. The space group for **3d** was determined on the basis of systematic absences and intensity statistics, and the structure of **3d** was solved by direct methods using SIR92 or SIR97 and refined with SHELXL-97. Selected crystallographic data for **3d** are given in [Supplementary data](#).

## 5.3. General procedure I: Preparation of compounds (2a–2l)

To a solution of diflunisal (0.9 g, 4 mmol) in anhydrous tetrahydrofuran (30 mL) was added dropwise thionyl chloride (1 mL, 14 mmol), and the mixture was refluxed under nitrogen atmosphere for 6 h. After cooling to room temperature, the mixture was steamed to give the intermediate by Dean–Stark apparatus. The residue was carried onto the next step without further purification and it was directly reacted with various anilines (4 mmol) in anhydrous tetrahydrofuran (30 mL) for 12–14 h. After removal of tetrahydrofuran, the reaction mixture was washed with ethyl acetate/*n*-hexane and the crude product was extracted with ethyl acetate (3 × 25 mL), washed with 10% NaHCO<sub>3</sub> (15 mL), H<sub>2</sub>O (3 × 25 mL), brine (10 mL), and then dried over anhydrous MgSO<sub>4</sub>. The organic layer was collected and concentrated in vacuo. The crude product was washed and purified by crystallization from hot ethanol to obtain compounds (**2a–2l**). The physicochemical characterizations of intermediates **2a–2l** are reported in the literature.<sup>60</sup>

## 5.4. General procedure II: Preparation of compounds (3a–3l)

A solution of methyl chloroformate (1.2 mL, 12 mmol) was added to a solution of compounds (**2a–2l**) (4 mmol) in dry anhydrous tetrahydrofuran/pyridine (30 mL) at 0 °C for 0.5 h. The following mixture was refluxed for 2 h and then stirred at room temperature upon completion. The reaction was adjusted to pH = 6 by 5% HCl<sub>(aq)</sub>. The mixture was cooled to obtain precipitated product under ice bath for 2–3 h. And then, precipitated crystals were filtered off and washed with diluted H<sub>2</sub>O/HCl<sub>(aq)</sub>. The crude product was purified by crystallization from hot ethanol to afford compounds (**3a–3l**).

### 5.4.1. 3-(4-Chloro-2-fluorophenyl)-6-(2,4-difluorophenyl)-2H-benzo[e][1,3]oxazine-2,4(3H)-dione (3a)

The pure compound was obtained as white powder (yield 11%). Mp: 176–177 °C (EtOH); <sup>1</sup>H NMR (300 MHz, DMSO-*d*<sub>6</sub>):  $\delta$  ppm 7.23

(td, *J* = 8.4, 2.5 Hz, 1H), 7.23 (td, *J* = 10.4, 2.7 Hz, 1H), 7.48–7.52 (m, 1H), 7.63–7.75 (m, 4H), 8.05 (dt, *J* = 8.4, 1.5 Hz, 1H), 8.10 (t, *J* = 1.8 Hz, 1H); <sup>13</sup>C NMR (75 MHz, DMSO-*d*<sub>6</sub>):  $\delta$  ppm 104.47, 104.74, 105.00, 112.26, 112.30, 112.47, 112.51, 114.34, 117.00, 117.23, 117.30, 121.26, 121.39, 122.63, 122.67, 122.76, 122.80, 125.50, 125.54, 127.25, 127.28, 131.62, 131.99, 132.03, 132.09, 134.89, 134.99, 137.17, 146.64, 152.12, 156.15, 157.85, 157.98, 158.67, 159.73, 160.33, 160.46, 160.87, 160.99, 163.34; HPLC purity: >95%; *t*<sub>R</sub> = 3.80 min; HRMS (EI) *m/z*: calcd [M]<sup>+</sup>, 403.0223 (C<sub>20</sub>H<sub>9</sub>ClF<sub>3</sub>NO<sub>3</sub><sup>+</sup>), found, 403.0229.

### 5.4.2. 3,6-Bis(2,4-difluorophenyl)-2H-benzo[e][1,3]oxazine-2,4(3H)-dione (3b)

The pure compound was obtained as white powder (yield 61%). Mp: 155–156 °C (EtOH); <sup>1</sup>H NMR (300 MHz, DMSO-*d*<sub>6</sub>):  $\delta$  ppm 7.20–7.33 (m, 2H), 7.42 (td, *J* = 9.7, 1.5 Hz, 1H), 7.54 (td, *J* = 9.7, 2.1 Hz, 1H), 7.65–7.74 (m, 3H), 8.03–8.10 (m, 2H); <sup>13</sup>C NMR (75 MHz, DMSO-*d*<sub>6</sub>):  $\delta$  ppm 104.38, 104.62, 104.74, 104.93, 104.98, 105.09, 105.29, 112.25, 112.53, 114.41, 117.34, 118.73, 118.85, 112.70, 112.87, 127.34, 131.75, 132.02, 132.07, 132.15, 132.20, 132.26, 137.21, 152.24, 156.10, 156.28, 157.74, 159.45, 159.94, 160.85, 161.04, 164.30; HPLC purity: >95%; *t*<sub>R</sub> = 4.71 min; HRMS (EI) *m/z*: calcd [M]<sup>+</sup>, 387.0519 (C<sub>20</sub>H<sub>9</sub>F<sub>4</sub>NO<sub>3</sub><sup>+</sup>), found, 387.0518.

### 5.4.3. 6-(2,4-Difluorophenyl)-3-(3,4-difluorophenyl)-2H-benzo[e][1,3]oxazine-2,4(3H)-dione (3c)

The pure compound was obtained as white powder (yield 25%). Mp: 193–194 °C (EtOH); <sup>1</sup>H NMR (300 MHz, DMSO-*d*<sub>6</sub>):  $\delta$  ppm 7.20–7.23 (m, 1H), 7.34–7.45 (m, 2H), 7.57–7.73 (m, 4H), 8.03–8.04 (m, 1H), 8.08 (t, *J* = 1.8 Hz, 1H); <sup>13</sup>C NMR (75 MHz, DMSO-*d*<sub>6</sub>):  $\delta$  ppm 104.48, 104.74, 105.00, 112.26, 112.29, 112.47, 112.51, 114.96, 117.10, 117.81, 117.99, 118.20, 118.39, 122.73, 122.76, 112.86, 122.89, 126.18, 126.21, 126.25, 126.28, 127.15, 127.18, 131.34, 131.59, 131.62, 131.67, 131.71, 131.94, 131.98, 132.04, 132.08, 136.74, 147.31, 147.92, 148.04, 148.33, 148.45, 150.37, 150.49, 150.79, 150.91, 152.05, 157.85, 157.98, 160.33, 160.42, 160.46, 160.84, 160.97, 163.31, 163.43; HPLC purity: >95%; *t*<sub>R</sub> = 4.56 min; HRMS (EI) *m/z*: calcd [M]<sup>+</sup>, 387.0519 (C<sub>20</sub>H<sub>9</sub>F<sub>4</sub>NO<sub>3</sub><sup>+</sup>), found, 387.0522.

### 5.4.4. 6-(2,4-Difluorophenyl)-3-(2,5-difluorophenyl)-2H-benzo[e][1,3]oxazine-2,4(3H)-dione (3d)

The pure compound was obtained as white powder (yield 15%). Mp: 144–145 °C (EtOH); <sup>1</sup>H NMR (300 MHz, DMSO-*d*<sub>6</sub>):  $\delta$  ppm 7.23 (td, *J* = 8.4, 2.4 Hz, 1H), 7.37–7.58 (m, 4H), 7.65–7.73 (m, 2H), 8.03–8.11 (m, 2H); <sup>13</sup>C NMR (75 MHz, DMSO-*d*<sub>6</sub>):  $\delta$  ppm 104.38, 104.74, 105.09, 112.25, 112.30, 112.53, 112.59, 114.32, 114.36, 117.39, 117.45, 117.50, 117.58, 117.75, 117.85, 118.06, 118.16, 118.37, 118.48, 122.66, 122.71, 122.87, 123.02, 123.08, 123.22, 127.37, 127.41, 131.86, 132.02, 132.07, 132.15, 132.20, 137.32, 137.35, 146.64, 152.21, 152.64, 155.95, 156.21, 157.60, 157.76, 159.40, 159.75, 160.63, 160.79, 160.91, 161.07, 163.92, 164.09; HPLC purity: >95%; *t*<sub>R</sub> = 3.90 min; HRMS (EI) *m/z*: calcd [M]<sup>+</sup>, 387.0519 (C<sub>20</sub>H<sub>9</sub>F<sub>4</sub>NO<sub>3</sub><sup>+</sup>), found, 387.0516.

#### 5.4.5. 6-(2,4-Difluorophenyl)-3-(2-(trifluoromethyl)phenyl)-2H-benzo[e][1,3]oxazine-2,4(3H)-dione (3e)

The pure compound was obtained as light orange powder (yield 31%). Mp: 200–201 °C (EtOH); <sup>1</sup>H NMR (300 MHz, DMSO-*d*<sub>6</sub>): δ ppm 7.23 (td, *J* = 9.3, 2.4 Hz, 1H), 7.42 (td, *J* = 10.2, 2.4 Hz, 1H), 7.68–7.82 (m, 4H), 7.89–7.95 (m, 2H), 8.05–8.11 (m, 2H); <sup>13</sup>C NMR (75 MHz, DMSO-*d*<sub>6</sub>): δ ppm 104.35, 104.70, 105.04, 112.21, 112.25, 112.53, 112.55, 114.31, 114.36, 117.38, 121.36, 122.64, 122.68, 122.80, 122.84, 124.90, 126.50, 126.92, 127.14, 127.30, 130.43, 131.55, 131.90, 132.06, 132.11, 132.19, 132.24, 132.70, 134.23, 137.35, 146.98, 152.15, 157.56, 157.63, 160.39, 161.04, 162.61, 162.74; HPLC purity: >95%; *t*<sub>R</sub> = 4.47 min; HRMS (EI) *m/z*: calcd [M]<sup>+</sup>, 419.0581 (C<sub>21</sub>H<sub>10</sub>F<sub>5</sub>NO<sub>3</sub><sup>+</sup>), found, 419.0586.

#### 5.4.6. 6-(2,4-Difluorophenyl)-3-(3-(trifluoromethyl)phenyl)-2H-benzo[e][1,3]oxazine-2,4(3H)-dione (3f)

The pure compound was obtained as white powder (yield 13%). Mp: 165–166 °C (EtOH); <sup>1</sup>H NMR (300 MHz, DMSO-*d*<sub>6</sub>): δ ppm 7.24 (td, *J* = 7.5, 2.1 Hz, 1H), 7.42 (td, *J* = 10.1, 2.7 Hz, 1H), 7.64–7.73 (m, 2H), 7.78–7.80 (m, 2H), 7.85–7.88 (m, 1H), 7.91 (s, 1H), 8.03 (dt, *J* = 9.3, 1.5 Hz, 1H), 8.08 (t, *J* = 1.8 Hz, 1H); <sup>13</sup>C NMR (75 MHz, DMSO-*d*<sub>6</sub>): δ ppm 104.48, 104.74, 105.00, 112.26, 112.29, 112.47, 112.51, 115.03, 117.10, 119.73, 122.44, 122.74, 122.78, 122.88, 122.91, 125.15, 125.70, 125.74, 127.13, 127.16, 127.86, 129.38, 129.70, 130.02, 130.34, 130.48, 131.31, 131.93, 131.97, 132.03, 132.07, 133.10, 135.98, 136.72, 147.41, 152.12, 157.86, 157.98, 160.33, 160.46, 160.53, 160.84, 160.96, 163.30, 163.43; HPLC purity: >95%; *t*<sub>R</sub> = 3.79 min; HRMS (EI) *m/z*: calcd [M]<sup>+</sup>, 419.0581 (C<sub>21</sub>H<sub>10</sub>F<sub>5</sub>NO<sub>3</sub><sup>+</sup>), found, 419.0590.

#### 5.4.7. 6-(2,4-Difluorophenyl)-3-(4-(trifluoromethyl)phenyl)-2H-benzo[e][1,3]oxazine-2,4(3H)-dione (3g)

The pure compound was obtained as white powder (yield 11%). Mp: 209–210 °C (EtOH); <sup>1</sup>H NMR (300 MHz, DMSO-*d*<sub>6</sub>): δ ppm 7.24 (td, *J* = 9, 1.2 Hz, 1H), 7.42 (td, *J* = 10.2, 2.4 Hz, 1H), 7.63–7.73 (m, 4H), 7.93 (d, *J* = 8.4 Hz, 2H), 8.03 (dt, *J* = 8.7, 2.1 Hz, 1H), 8.08 (t, *J* = 1.5 Hz, 1H); <sup>13</sup>C NMR (75 MHz, DMSO-*d*<sub>6</sub>): δ ppm 105.00, 105.35, 105.70, 112.85, 112.90, 113.13, 113.18, 115.74, 117.77, 122.86, 123.43, 123.48, 123.66, 126.48, 126.93, 126.97, 127.83, 127.87, 129.88, 130.30, 130.54, 132.06, 132.59, 132.65, 132.72, 132.78, 137.41, 139.60, 147.97, 152.91, 158.26, 158.36, 161.15, 161.68, 163.72, 164.64; HPLC purity: >95%; *t*<sub>R</sub> = 4.71 min; HRMS (EI) *m/z*: calcd [M]<sup>+</sup>, 419.0581 (C<sub>21</sub>H<sub>10</sub>F<sub>5</sub>NO<sub>3</sub><sup>+</sup>), found, 419.0584.

#### 5.4.8. 6-(2,4-Difluorophenyl)-3-(3-ethynylphenyl)-2H-benzo[e][1,3]oxazine-2,4(3H)-dione (3h)

The pure compound was obtained as light orange crystal (yield 14%). Mp: 195–196 °C (EtOH); <sup>1</sup>H NMR (300 MHz, DMSO-*d*<sub>6</sub>): δ ppm 4.29 (s, 1H), 7.23 (td, *J* = 8.3, 2.7 Hz, 1H), 7.42 (td, *J* = 10.2, 2.4 Hz, 1H), 7.48–7.73 (m, 6H), 7.99–8.04 (m, 1H), 8.07 (t, *J* = 1.8 Hz, 1H); <sup>13</sup>C NMR (75 MHz, DMSO-*d*<sub>6</sub>): δ ppm 81.64, 82.42, 104.38, 104.73, 105.08, 112.23, 112.28, 112.51, 112.56, 115.11, 117.12, 122.60, 122.87, 122.99, 123.05, 127.26, 129.49, 129.56, 129.67, 131.39, 131.92, 131.98, 132.09, 132.15, 132.20, 135.54, 136.72, 147.46, 152.25, 157.57, 157.73, 160.55, 160.87, 161.04; HPLC purity: >95%; *t*<sub>R</sub> = 4.44 min; HRMS (EI) *m/z*: calcd [M]<sup>+</sup>, 375.0707 (C<sub>22</sub>H<sub>11</sub>F<sub>2</sub>NO<sub>3</sub><sup>+</sup>), found, 375.0708.

#### 5.4.9. 3-(6-(2,4-Difluorophenyl)-2,4-dioxo-2H-benzo[e][1,3]-oxazin-3(4H)-yl)benzotrile (3i)

The pure compound was obtained as brown powder (yield 49%). Mp: 209–210 °C (EtOH); <sup>1</sup>H NMR (300 MHz, DMSO-*d*<sub>6</sub>): δ ppm 7.21–7.27 (m, 1H), 7.42 (td, *J* = 10.5, 2.4 Hz, 1H), 7.64–7.86 (m, 5H), 7.96–8.05 (m, 2H), 8.09 (t, *J* = 1.8 Hz, 1H); <sup>13</sup>C NMR (75 MHz, DMSO-*d*<sub>6</sub>): δ ppm 104.24, 104.50, 104.76, 111.62, 111.91, 111.95, 112.12, 112.16, 117.50, 118.40, 118.66, 123.51, 123.97, 124.01, 124.11, 124.14, 125.23, 125.31, 127.61, 129.54, 130.22, 131.58,

131.62, 131.67, 131.72, 133.97, 134.00, 139.13, 157.59, 157.74, 157.87, 160.21, 160.33, 162.66, 162.78, 166.25; HPLC purity: >95%; *t*<sub>R</sub> = 8.43 min; HRMS (EI) *m/z*: calcd [M]<sup>+</sup>, 376.0659 (C<sub>21</sub>H<sub>10</sub>F<sub>2</sub>N<sub>2</sub>O<sub>3</sub><sup>+</sup>), found, 375.0622.

#### 5.4.10. 4-(6-(2,4-Difluorophenyl)-2,4-dioxo-2H-benzo[e][1,3]-oxazin-3(4H)-yl)benzotrile (3j)

The pure compound was obtained as yellowish brown powder (yield 22%). Mp: 203–204 °C (EtOH); <sup>1</sup>H NMR (300 MHz, DMSO-*d*<sub>6</sub>): δ ppm 7.24 (td, *J* = 8.7, 0.9 Hz, 1H), 7.42 (td, *J* = 10.1, 2.7 Hz, 1H), 7.63–7.73 (m, 4H), 8.01–8.08 (m, 4H); <sup>13</sup>C NMR (75 MHz, DMSO-*d*<sub>6</sub>): δ ppm 104.37, 104.72, 105.07, 111.91, 112.27, 112.51, 112.56, 115.05, 117.15, 118.32, 122.82, 122.95, 127.19, 130.14, 131.46, 131.96, 132.01, 132.08, 132.14, 133.35, 136.83, 139.47, 147.19, 152.24, 160.40, 163.97, 164.12; HPLC purity: >95%; *t*<sub>R</sub> = 3.48 min; HRMS (EI) *m/z*: calcd [M]<sup>+</sup>, 376.0659 (C<sub>21</sub>H<sub>10</sub>F<sub>2</sub>N<sub>2</sub>O<sub>3</sub><sup>+</sup>), found, 375.0655.

#### 5.4.11. 6-(2,4-Difluorophenyl)-3-(3,4-dimethoxyphenyl)-2H-benzo[e][1,3]oxazine-2,4(3H)-dione (3k)

The pure compound was obtained as white powder (yield 43%). Mp: 198–199 °C (EtOH); <sup>1</sup>H NMR (300 MHz, DMSO-*d*<sub>6</sub>): δ ppm 3.72 (s, 3H), 3.81 (s, 3H), 6.96 (dd, *J* = 8.5, 2.1 Hz, 1H), 7.04–7.09 (m, 2H), 7.20–7.27 (m, 1H), 7.42 (td, *J* = 8.3, 2.7 Hz, 1H), 7.61 (d, *J* = 8.4 Hz, 1H), 7.65–7.73 (m, 1H), 7.98–8.02 (m, 1H), 8.07 (t, *J* = 1.5 Hz, 1H); <sup>13</sup>C NMR (75 MHz, DMSO-*d*<sub>6</sub>): δ ppm 55.63, 55.68, 104.13, 104.48, 104.83, 111.95, 112.27, 112.32, 112.70, 114.97, 116.81, 120.78, 127.15, 127.78, 131.17, 131.74, 131.79, 13.87, 131.93, 136.37, 147.49, 149.10, 149.16, 152.07, 157.74, 160.48, 160.90, 161.15, 164.26; HPLC purity: >95%; *t*<sub>R</sub> = 3.42 min; HRMS (EI) *m/z*: calcd [M]<sup>+</sup>, 411.0918 (C<sub>22</sub>H<sub>15</sub>F<sub>2</sub>NO<sub>5</sub><sup>+</sup>), found, 411.0917.

#### 5.4.12. 6-(2,4-Difluorophenyl)-3-(3-methoxyphenyl)-2H-benzo[e][1,3]oxazine-2,4(3H)-dione (3l)

The pure compound was obtained as light orange powder (yield 12%). Mp: 160–161 °C (EtOH); <sup>1</sup>H NMR (300 MHz, DMSO-*d*<sub>6</sub>): δ ppm 3.77 (s, 3H), 6.99–7.07 (m, 2H), 7.20–7.27 (m, 1H), 7.38–7.45 (m, 2H), 7.23–7.60 (m, 2H), 7.98–8.03 (m, 1H), 8.07 (t, *J* = 1.8 Hz, 1H); <sup>13</sup>C NMR (75 MHz, DMSO-*d*<sub>6</sub>): δ ppm 55.18, 104.13, 104.48, 104.83, 112.03, 112.26, 112.31, 114.36, 114.44, 114.97, 116.84, 120.61, 122.70, 127.11, 129.59, 131.20, 131.79, 131.86, 131.92, 136.12, 136.41, 147.21, 152.10, 152.40, 159.79, 160.27, 162.73, 164.16; HPLC purity: >95%; *t*<sub>R</sub> = 3.92 min; HRMS (EI) *m/z*: calcd [M]<sup>+</sup>, 381.0813 (C<sub>21</sub>H<sub>13</sub>F<sub>2</sub>NO<sub>4</sub><sup>+</sup>), found, 381.0806.

## 5.5. Biological materials

RAW264.7 murine monocyte/macrophage cells was obtained from American Type Culture Collection (ATCC, Rockville, MD, USA); Receptor activator of nuclear factor kappa-B ligand (RANKL, Peprotech, Inc., London, UK); Specific monoclonal primary antibodies NF-κB (Clone code: E379, Epitomics, Inc., CA, USA); NFATc1 (Clone code: 7A6, Santa Cruz Biotechnology, Santa Cruz Inc., CA, USA); TATA box-binding protein (Clone code: 1TBP18, Abcam Inc., Cambridge, MA, USA); NE-PER nuclear and cytoplasmic extraction reagents (Thermo Fisher Scientific, USA); Unless otherwise stated, all materials and assay kits were used from commercially available. Chemical reagents were purchased from Sigma-Aldrich without further purification.

### 5.5.1. Cell culture

RAW264.7 murine monocyte/macrophage cells were obtained from American Type Culture Collection (ATCC, Rockville, MD, USA). These cells were cultured with Dulbecco's Modified Eagle Medium (DMEM, Gibco BRL, NY, USA) and supplemented with

10% heat-inactivated fetal bovine serum (FBS) in 95% air, 5% CO<sub>2</sub> humid atmosphere at 37 °C.

### 5.5.2. Cell viability assay<sup>41,53</sup>

RAW264.7 cells were seeded into a 96-well culture plate at a density of  $1 \times 10^4$  per well with 200  $\mu$ L medium (DMEM) supplemented with 10% FBS and treated with a series of synthesized compounds for 24 h. After 24 h, 96-well plate were washed three times with phosphate-buffered saline ( $3 \times$  PBS) and then treated with medium containing 500  $\mu$ g/mL of 3-(4,5-dimethylthiazol-2-yl)-2,5-diphenyltetrazolium bromide (MTT) reagent for 1 h at 37 °C. Cells were then washed with PBS and solubilized in 100  $\mu$ L of DMSO. MTT reagent was designed to yield a formazan by metabolic reduction of viable cells. Absorbance was measured at 540 nm by using an ELISA reader.

### 5.5.3. Tartrate-resistant acid phosphatase (TRAP) staining assay<sup>41</sup>

RAW264.7 cells were seeded into 96-well culture plate at a density of  $1 \times 10^3$  per well and/or seeded into 48-well plate at a density of  $2 \times 10^4$  cells per well with  $\alpha$ -MEM Essential Medium ( $\alpha$ -MEM, Gibco BRL, NY, USA) containing 10% FBS, 2 mM L-glutamate, 100 ng/mL of recombinant soluble murine RANKL (Peprotech, London, UK) in the presence with or without tested compounds. Cell cultures were incubated with 95% air, 5% CO<sub>2</sub> at 37 °C for 4 days. Cell culture media (containing the test compounds) were changed on day 2. After 4 days, cells were washed with PBS and fixed with solution (acetone/citrate solution/37% formaldehyde, 65:25:8) for 30 min. And then, cells were incubated with light-protected incubator at 37 °C for 1 h by using the Leukocyte Acid Phosphatase Assay kit (Cat.387A, Sigma). Cells were washed three times with distilled water and TRAP-positive multinucleated cells containing three or more than three nuclei ( $N > 3$ ) were counted under a light microscope and photographed.

### 5.5.4. Tartrate-resistant acid phosphatase (TRAP) activity assay<sup>41,53</sup>

RAW264.7 cells were seeded into 48-well plate at a density of  $2 \times 10^4$  cells per well with  $\alpha$ -MEM medium containing 10% FBS, 2 mM L-glutamate, 100 ng/mL of recombinant soluble murine RANKL in the presence with or without tested compounds. For the measurement of TRAP activity, the cells were washed with phosphate-buffered saline (PBS) on 4 day, and then 100  $\mu$ L of lysis solution (0.1% Triton X-100 in 50 mM Tris-HCl, pH = 7.2) was added to each well for 15 min under ice-bath. Subsequently, the 100  $\mu$ L of substrate solution (2 mg/mL 4-nitrophenyl phosphate in 0.09 M citrate buffer, Sigma Chemical Co.) was added to each well and incubated for 15 min at 37 °C. The reaction was stopped by adding 200  $\mu$ L of 0.1 N NaOH<sub>(aq)</sub> and transferred 100  $\mu$ L mixtures into 96-well plates. Absorbance was measured at 405 nm by using an ELISA reader. The intracellular protein level was measured at 562 nm by using a BCA protein assay kit (Pierce, USA).

### 5.5.5. Reverse transcription polymerase chain reaction (RT-PCR) analysis<sup>41,53</sup>

RAW264.7 cells were seeded into 6-cm dish at a density of  $1 \times 10^5$  cells per well with DMEM medium containing 10% FBS. After 1 day, cells were starved for 24 h by replacing DMEM medium to  $\alpha$ -MEM medium, 100 ng/mL of recombinant soluble murine RANKL in the presence with or without the test compounds for 24 h. Total RNA was isolated from cultured cells with Trizol reagent (Invitrogen). The RNA (2  $\mu$ g) was reversibly transcribed with SuperScript II reverse transcriptase (Invitrogen) and oligo-(dT)<sub>15</sub> primer. The cDNA was amplified using mouse-specific primer (Table 2). The PCR was performed in 25  $\mu$ L of 10 mM Tris-HCl (pH = 8.8), 1.5 mM MgCl<sub>2</sub>, 50 mM KCl, 0.1% Triton

X-100, 1 unit DNA polymerase (Protech), 200  $\mu$ M dNTP and 10  $\mu$ M primer. PCR products were separated on 1.5% agarose gels, and the bands were visualized by ethidium bromide staining (EtBr). The optical densities for each gene were normalized to the corresponding values for glyceraldehyde-3-phosphate dehydrogenase (GAPDH).

### 5.5.6. Western blotting assay<sup>41,53</sup>

RAW264.7 cells were seeded into 6-cm dish at a density of  $1 \times 10^5$  cells per well with DMEM medium containing 10% FBS for 24 h. And then, the cells were pretreated with the test compounds in  $\alpha$ -MEM medium containing 10% FBS for 1 h prior to treatment with RANKL (100 ng/mL) for 24 h. After 1 day, the cells were washed three times with PBS. Nuclear extracts were collected by NE-PER Nuclear and Cytoplasmic Extraction Kit (Cat. 78833, Thermo Scientific, USA) according to the manufacturer's instructions. Then, equivalent amounts of nuclear protein extracts (18  $\mu$ g) protein were loaded for 12% SDS-PAGE gels and transferred to immobilon polyvinylidene difluoride members. Non-specific binding was blocked by soaking members in the TBS buffer containing 5% BSA for 1 h. The blots were probed with specific monoclonal primary antibodies (mAb, 1:1000), such as NF- $\kappa$ B (Clone code: E379, Epitomics, Inc., CA, USA), NFATc1 (Clone code: 7A6, Santa Cruz Biotechnology, Santa Cruz, CA, USA), and TATA box-binding protein (TBP, Clone code: 1TBP18, Abcam Inc., Cambridge, MA, USA) for 12 h at 4 °C. After further washing by TBST, the blots were subsequently incubated with a secondary antibody coupled to horseradish-peroxidase (a goat anti-rabbit IgG, 1:10,000) for 1 h. The immunoreactive bands were visualized by using the Immobilon Western Chemiluminescent HRP Substrate kit (Millipore) and by exposing a clear Blue X-ray film (Thermo Fisher Scientific, USA) to the membrane.

### 5.5.7. NF- $\kappa$ B activity assay<sup>60</sup>

RAW264.7 cells were seeded into 6-cm dish at a density of  $1 \times 10^5$  cells per well with DMEM medium containing 10% FBS for 24 h. And then, the cells were pretreated with the test compounds in  $\alpha$ -MEM medium containing 10% FBS for 1 h prior to treatment with RANKL (100 ng/mL) for 24 h. After 1 day, the cells were washed three times with PBS. Nuclear extracts were collected by NE-PER Nuclear and Cytoplasmic Extraction Kit (Cat. 78833, Thermo Scientific, USA). NF- $\kappa$ B translocation was determined by using a Cayman Chemical NF- $\kappa$ B (p65) kit (Cat. 10007889), a sensitive method for the detection of specific transcription factor DNA binding activity in nuclear extracts. This assay is used to analyze the NF- $\kappa$ B activity or transactivation potential, as NF- $\kappa$ B binds to the response element pre-coated on specific ELISA plates, a primary antibody followed by a tagged secondary antibody is then added. Absorbance is read at 450 nm which correlates with NF- $\kappa$ B activity.

### 5.5.8. Resorbing activity of osteoclasts by bone resorption assay<sup>41</sup>

RAW264.7 cells were seeded into dentine slices (24-well plates, Corning) at a density of  $1 \times 10^4$  cells per well with  $\alpha$ -MEM medium (containing 10% FBS, 2 mM L-glutamate), 100 ng/mL of recombinant soluble murine RANKL in the presence with or without the test compounds. All cultured cells were replenished every 2 days with fresh medium containing tested chemicals. After 4 days, the wells were washed three times with PBS, left in 1 M ammonium hydroxide to remove the attached cells and stained with 0.1% toluidine blue (Sigma Chemical Co.). In optical field on a slice, the ratios of the resorbed area to the total area were measured by using the ImageJ software.

## Acknowledgments

The present study was supported by the National Science Council Grant (NSC 101-2113-M-016-001), Ministry of Science and Technology (MOST 102-2314-B-075-083-MY3), and Taipei Medical University (TMU 102-AE1-B32). We also thank Ting-Shen Kuo for kindly providing the information of crystallography.

## Supplementary data

Supplementary data (inhibitory effects of compounds on RANKL-induced osteoclastogenesis; spectroscopic characterizations ( $^1\text{H}$  NMR,  $^{13}\text{C}$  NMR and HRMS spectra) of compounds; purity of final compounds; crystallographic data) associated with this article can be found, in the online version, at <http://dx.doi.org/10.1016/j.bmc.2015.06.007>.

## References and notes

- Sims, N. A.; Gooi, J. H. *Semin. Cell Dev. Biol.* **2008**, *19*, 444.
- Crockett, J. C.; Rogers, M. J.; Coxon, F. P.; Hocking, L. J.; Helfrich, M. H. *J. Cell Sci.* **2011**, *124*, 991.
- Martin, T. J.; Sims, N. A. *Trends Mol. Med.* **2005**, *11*, 76.
- Kong, Y. Y.; Penninger, J. M. *Exp. Gerontol.* **2000**, *35*, 947.
- Seeman, E. *Lancet* **2002**, *359*, 1841.
- McInnes, I. B.; Schett, G. *N. Eng. J. Med.* **2011**, *365*, 2205.
- Okamoto, K.; Takayanagi, H. *Int. Immunopharmacol.* **2011**, *11*, 543.
- Takayanagi, H.; Iizuka, H.; Juji, T.; Nakagawa, T.; Yamamoto, A.; Miyazaki, T.; Koshihara, Y.; Oda, H.; Nakamura, K.; Tanaka, S. *Arthritis Rheum.* **2000**, *43*, 259.
- Boyle, W. J.; Simonet, W. S.; Lacey, D. L. *Nature* **2003**, *423*, 337.
- Fujikawa, Y.; Quinn, J. M.; Sabokbar, A.; McGee, J. O.; Athanasou, N. A. *Endocrinology* **1996**, *137*, 4058.
- Teitelbaum, S. L.; Ross, F. P. *Nat. Rev. Genet.* **2003**, *4*, 638.
- Udagawa, N.; Takahashi, N.; Akatsu, T.; Tanaka, H.; Sasaki, T.; Nishihara, T.; Koga, T.; Martin, T. J.; Suda, T. *Proc. Natl. Acad. Sci. U.S.A.* **1990**, *87*, 7260.
- Suda, T.; Takahashi, N.; Udagawa, N.; Jimi, E.; Gillespie, M. T.; Martin, T. J. *Endocr. Rev.* **1999**, *20*, 345.
- Wong, B. R.; Josien, R.; Lee, S. Y.; Vologodskaja, M.; Steinman, R. M.; Choi, Y. *J. Biol. Chem.* **1998**, *273*, 28355.
- Yasuda, H.; Shima, N.; Nakagawa, N.; Yamaguchi, K.; Kinosaki, M.; Mochizuki, S.; Tomoyasu, A.; Yano, K.; Goto, M.; Murakami, A.; Tsuda, E.; Morinaga, T.; Higashio, K.; Udagawa, N.; Takahashi, N.; Suda, T. *Proc. Natl. Acad. Sci. U.S.A.* **1998**, *95*, 3597.
- Dougall, W. C.; Glaccum, M.; Charrier, K.; Rohrbach, K.; Brasel, K.; De Smedt, T.; Daro, E.; Smith, J.; Tometsko, M. E.; Maliszewski, C. R.; Armstrong, A.; Shen, V.; Bain, S.; Cosman, D.; Anderson, D.; Morrissey, P. J.; Peschon, J. J.; Schuh, J. *Genes Dev.* **1999**, *13*, 2412.
- Nakao, A.; Fukushima, H.; Kajiya, H.; Ozeki, S.; Okabe, K. *Biochem. Biophys. Res. Commun.* **2007**, *357*, 945.
- Asagiri, M.; Sato, K.; Usami, T.; Ochi, S.; Nishina, H.; Yoshida, H.; Morita, I.; Wagner, E. F.; Mak, T. W.; Serfling, E.; Takayanagi, H. *J. Exp. Med.* **2005**, *202*, 1261.
- Matsuo, K.; Galson, D. L.; Zhao, C.; Peng, L.; Laplace, C.; Wang, K. Z.; Bachler, M. A.; Amano, H.; Aburatani, H.; Ishikawa, H.; Wagner, E. F. *J. Biol. Chem.* **2004**, *279*, 26475.
- Zhou, B.; Cron, R. Q.; Wu, B.; Genin, A.; Wang, Z.; Liu, S.; Robson, P.; Baldwin, H. S. *J. Biol. Chem.* **2002**, *277*, 10704.
- Grigoriadis, A. E.; Wang, Z. Q.; Cecchini, M. G.; Hofstetter, W.; Felix, R.; Fleisch, H. A.; Wagner, E. F. *Science* **1994**, *266*, 443.
- Wang, Z. Q.; Ovitt, C.; Grigoriadis, A. E.; Mohle-Steinlein, U.; Ruther, U.; Wagner, E. F. *Nature* **1992**, *360*, 741.
- Hayman, A. R.; Jones, S. J.; Boyde, A.; Foster, D.; Colledge, W. H.; Carlton, M. B.; Evans, M. J.; Cox, T. M. *Development* **1996**, *122*, 3151.
- Hollberg, K.; Hultenby, K.; Hayman, A.; Cox, T.; Andersson, G. *Exp. Cell Res.* **2002**, *279*, 227.
- Matsumoto, M.; Kogawa, M.; Wada, S.; Takayanagi, H.; Tsujimoto, M.; Katayama, S.; Hisatake, K.; Nogi, Y. *J. Biol. Chem.* **2004**, *279*, 45969.
- Saftig, P.; Hunziker, E.; Everts, V.; Jones, S.; Boyde, A.; Wehmeyer, O.; Suter, A.; von Figura, K. *Adv. Exp. Med. Biol.* **2000**, *477*, 293.
- Delaisse, J. M.; Andersen, T. L.; Engsig, M. T.; Henriksen, K.; Troen, T.; Blavier, L. *Microsc. Res. Tech.* **2003**, *61*, 504.
- Ishibashi, O.; Niwa, S.; Kadoyama, K.; Inui, T. *Life Sci.* **2006**, *79*, 1657.
- Kukita, T.; Wada, N.; Kukita, A.; Kakimoto, T.; Sandra, F.; Toh, K.; Nagata, K.; Iijima, T.; Horiuchi, M.; Matsusaki, H.; Hieshima, K.; Yoshie, O.; Nomiya, H. *J. Exp. Med.* **2004**, *200*, 941.
- Yagi, M.; Miyamoto, T.; Sawatani, Y.; Iwamoto, K.; Hosogane, N.; Fujita, N.; Morita, K.; Ninomiya, K.; Suzuki, T.; Miyamoto, K.; Oike, Y.; Takeya, M.; Toyama, Y.; Suda, T. *J. Exp. Med.* **2005**, *202*, 345.
- Arantes, H. P.; Silva, A. G.; Lazaretti-Castro, M. *Arq. Bras. Endocrinol. Metabol.* **2010**, *54*, 206.
- Russell, R. G.; Watts, N. B.; Ebetino, F. H.; Rogers, M. J. *Osteoporos. Int.* **2008**, *19*, 733.
- Sato, M.; Grese, T. A.; Dodge, J. A.; Bryant, H. U.; Turner, C. H. *J. Med. Chem.* **1999**, *42*, 1.
- Conte, P.; Guarneri, V. *Oncologist* **2004**, *9*, 28.
- Strampel, W.; Emkey, R.; Civitelli, R. *Drug Saf.* **2007**, *30*, 755.
- Watts, N. B. *Clin. Geriatr. Med.* **2003**, *19*, 395.
- Tsai, H. Y.; Lin, H. Y.; Fong, Y. C.; Wu, J. B.; Chen, Y. F.; Tsuzuki, M.; Tang, C. H. *Eur. J. Pharmacol.* **2008**, *588*, 124.
- Tang, C. H.; Chang, C. S.; Tan, T. W.; Liu, S. C.; Liu, J. F. *Eur. J. Pharmacol.* **2010**, *648*, 59.
- Rassi, C. M.; Lieberherr, M.; Chaumaz, G.; Pointillart, A.; Cournot, G. *J. Bone Miner. Res.* **2002**, *17*, 630.
- Lu, S.-H.; Huang, R.-Y.; Chou, T.-C. *Evid. Based Complement Alternat. Med.* **2013**, *2013*, 12.
- Cheng, C. P.; Huang, H. S.; Hsu, Y. C.; Sheu, M. J.; Chang, D. M. *J. Clin. Immunol.* **2012**, *32*, 762.
- Chen, C. L.; Liu, F. L.; Lee, C. C.; Chen, T. C.; Ahmed Ali, A. A.; Sytwu, H. K.; Chang, D. M.; Huang, H. S. *J. Med. Chem.* **2014**, *57*, 8072.
- Coste, E.; Greig, I. R.; Mollat, P.; Rose, L.; Gray, M.; Ralston, S. H.; Van't Hof, R. J. *Ann. Rheum. Dis.* **2013**.
- Idris, A. I.; Coste, E.; Greig, I. R.; Ralston, S. H.; van't Hof, R. J. *Calcif. Tissue Int.* **2010**, *87*, 525.
- Greig, I. R.; Coste, E.; Ralston, S. H.; van't Hof, R. J. *Bioorg. Med. Chem. Lett.* **2013**, *23*, 816.
- Greig, I. R.; Idris, A. I.; Ralston, S. H.; van't Hof, R. J. *J. Med. Chem.* **2006**, *49*, 7487.
- Idris, A. I.; Greig, I. R.; Bassonga-Landao, E.; Ralston, S. H.; van't Hof, R. J. *Endocrinology* **2009**, *150*, 5.
- Idris, A. I.; Mrak, E.; Greig, I.; Guidobono, F.; Ralston, S. H.; van't Hof, R. J. *Biochem. Biophys. Res. Commun.* **2008**, *371*, 94.
- Van't Hof, R. J.; Idris, A. I.; Ridge, S. A.; Dunford, J.; Greig, I. R.; Ralston, S. H. *J. Bone Miner. Res.* **2004**, *19*, 1651.
- de Silva, M.; Hazleman, B. L.; Dippy, J. E. *Rheumatol. Rehabil.* **1980**, *19*, 126.
- Tempero, K. F.; Cirillo, V. J.; Steelman, S. L. *Br. J. Clin. Pharmacol.* **1977**, *4*, 31S.
- Skala, P.; Machacek, M.; Vejsova, M.; Kubcova, L.; Kunes, J.; Waisser, K. *J. Heterocycl. Chem.* **2009**, *46*, 873.
- Hsu, Y. C.; Cheng, C. P.; Chang, D. M. *J. Rheumatol.* **2011**, *38*, 1844.
- Igarashi, Y.; Lee, M. Y.; Matsuzaki, S. *J. Chromatogr., B Analyt. Technol. Biomed. Life Sci.* **2002**, *781*, 345.
- Asagiri, M.; Takayanagi, H. *Bone* **2007**, *40*, 251.
- Wada, T.; Nakashima, T.; Hiroshi, N.; Penninger, J. M. *Trends Mol. Med.* **2006**, *12*, 17.
- Yamashita, T.; Yao, Z.; Li, F.; Zhang, Q.; Badell, I. R.; Schwarz, E. M.; Takeshita, S.; Wagner, E. F.; Noda, M.; Matsuo, K.; Xing, L.; Boyce, B. F. *J. Biol. Chem.* **2007**, *282*, 18245.
- Lee, W. Z.; Chiang, C. W.; Kulkarni, G. M.; Kuo, T. S. *J. Chin. Chem. Soc.* **2013**, *60*, 245.
- Lee, W. Z.; Wang, T. L.; Chang, H. C.; Chen, Y. T.; Kuo, T. S. *Organometallics* **2012**, *31*, 4106.
- Lee, C. C.; Liu, F. L.; Chen, C. L.; Chen, T. C.; Chang, D. M.; Huang, H. S. *Eur. J. Med. Chem.* **2015**, *98*, 115.